

Systematics of Cluster-Radioactivity-Decay Constants as Suggested by Microscopic Calculations

R. Blendowske and H. Walliser

Fachbereich Physik, Universität Gesamthochschule Siegen, 59 Siegen, Federal Republic of Germany

(Received 27 July 1988)

In the microscopic approach the decay constant of cluster radioactivity is determined by the preformation probability for the open channel multiplied with the Gamov penetrability. The preformation probability is found to possess a simple mass dependence on the emitted cluster. This observation leads to a formula for order-of-magnitude estimates of absolute decay constants. The estimates are in excellent agreement with available experimental data. Predictions for as-yet unmeasured decay rates are made.

PACS numbers: 23.90.+w, 21.60.Gx, 27.90.+b

Since the discovery of the ^{14}C decay of ^{223}Ra by Rose and Jones in 1984, a number of similar decays have been reported.^{1,2} These radioactive decays with charge and mass numbers

$$(Z+z)(A+a) \rightarrow {}^z_a + {}^Z_A \quad (1)$$

emit clusters (z,a) , heavier than the α particle, such as the already measured ^{14}C , ^{24}Ne , and ^{28}Mg . The number of decays of this type which are experimentally accessible is limited. For energetical reasons, the fragment (z,a) should be even-even (pairing) and the daughter nucleus (Z,A) should lie in the stability valley, preferably close to the doubly magic ^{208}Pb . For experimental reasons, the parent nucleus $(Z+z, A+a)$ should have sufficiently long lifetime and hence should also lie in the "stability valley." This explains the neutron excess (corresponding to roughly $z/a \approx Z/A \approx 0.4$) found in the observed light fragments.

Because of the vivid experimental activity in the field, simple reliable estimates of decay constants of favorable decay modes are useful. In a microscopic study, cluster radioactive decays were successfully described as a gen-

eralization of the α -decay theory.³ Microscopic calculations, however, especially for heavier clusters, become rather involved. Fortunately, a very simple systematics is inherent in the microscopic theory. A formula for order-of-magnitude estimates of cluster-decay constants is readily extracted. This formula is intuitively understood and reproduces the available experimental data excellently. Predictions for a number of as-yet unmeasured decays are propounded.

In the microscopic approach, the decay constant is given as a product

$$\lambda = \lambda_G S. \quad (2)$$

The spectroscopic factor S represents the probability of the open-channel structure ${}^z_a + {}^Z_A$ to be preformed in the parent nucleus, and the Gamov decay constant λ_G describes the tunneling of the (preformed) cluster through the potential barrier in a naive Gamov picture. For a more detailed discussion of the physical assumptions leading to Eq. (2), see Ref. 4.

λ_G can be determined sufficiently accurate with use of the WKB approximation:

$$\lambda_G = \frac{v}{2R_i} P, \quad P = \exp \left\{ -2 \int_{R_i}^{R_o} dR \{ (2M/h^2) [U(R) - Q] \}^{1/2} \right\}, \quad (3)$$

where R_i and R_o are the inner and outer turning points, M is the reduced mass, and Q is the tunneling energy⁵ of the emitted cluster. For the prefactor $v/2R_i$, a kinetic energy $\frac{1}{2} M v^2 = 25a$ MeV is assumed inside the barrier. The potential used is a semiempirical heavy-ion potential

$$U(R) = - (50 \text{ MeV}/1 \text{ fm}) [R_a R_A / (R_a + R_A)] \exp[- (R - R_a - R_A)/d] + zZe^2/R, \quad (4)$$

$$R_x = (1.233x^{1/3} - 0.978x^{-1/3}) \text{ fm} \quad (x = a, A), \quad d = 0.63 \text{ fm},$$

fitted to elastic scattering⁶ (because the influence of the centrifugal potential is negligible, the angular momentum is set equal to zero). The penetrability (3) is sensitive to the outer tail only, therefore the results should not depend too much on the particular shape of the potential as long as scattering data are reasonably reproduced. Our choice is mainly due to practical reasons because the potential (4) is applicable to a whole variety of combinations ${}^z_a + {}^Z_A$.

The microscopic point of view enters specifically into the evaluation of the preformation probability by use of many-body wave functions. The large number of nucleons involved makes these calculations rather extensive, and it seems to be difficult to extend the procedure to clusters heavier than ^{16}O . In Fig. 1(a), some calculated spectroscopic factors for $a \leq 16$ are displayed (for even A in the lead region). The logarithmic plot, reveals

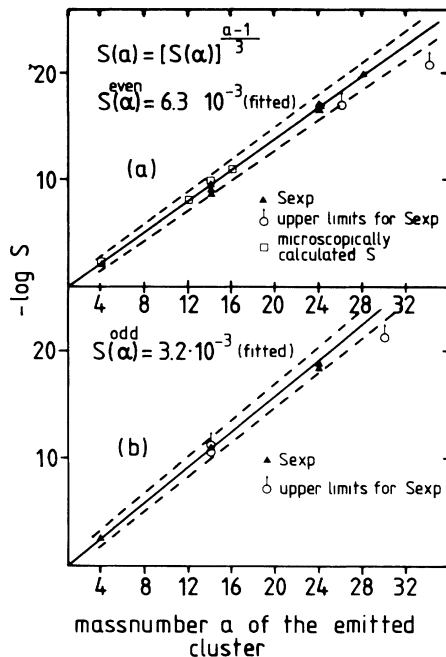


FIG. 1. Experimental spectroscopic factors are shown in a logarithmic plot for (a) even and (b) odd decay modes. Linear fits to the data are given by straight lines. Uncertainties as mentioned in the text are indicated by dotted lines. Some microscopically calculated spectroscopic factors are also shown in Fig. 1(a).

a nearly linear a dependence given by

$$S(a) = [S(\alpha)]^{(a-1)/3}. \quad (5)$$

This result is easy to understand. The preformation probability is given by overlaps of the nucleon states in the cluster with those of the parent nucleus.⁴ If we disregard normalization effects and the specific structure of the nuclei involved, the spectroscopic factor has to scale roughly with an exponent proportional to $(a-1)$ because effectively only the $(a-1)$ internal coordinates of the cluster contribute. For the α particle we have $a-1=3$ which explains the formula above (the nucleon spectroscopic factor is equal to 1 in this simple picture). In principle, $S(\alpha)$ can be taken from theory or experiment and there is no adjustable parameter for the estimation of the spectroscopic factor according to Eq. (5).

On the other hand, so-called experimental spectroscopic factors

$$S_{\text{expt}} = \lambda_{\text{expt}}/\lambda_G \quad (6)$$

can be extracted from known experimental decay constants. Since only quantities fixed by experiment enter the calculation, the variation of S_{expt} is itself an experimental information. For all measured decays, S_{expt} is

shown in the logarithmic plots of Fig. 1. The fact that spectroscopic factors for different decays but fixed mass number of the light fragment turn out to have similar values is certainly no accident. Also, the linear behavior up to relatively heavy clusters ($^2a = ^{28}\text{Mg}$) is surprising and strongly supports Eq. (5) and the underlying model. From Fig. 1 the well-known odd-even effect is noticed: Decays with even A (and $a+A$) are preferred.² Linear fits to the data (straight lines) yield the values

$$S^{\text{even}}(\alpha) = 6.3 \times 10^{-3}, \quad S^{\text{odd}}(\alpha) = 3.2 \times 10^{-3}, \quad (7)$$

which reflect this effect. The fitted numbers are in good agreement with experimental and theoretical α -spectroscopic factors in the Pb region (see Fig. 1). These values are used in Eq. (5) to calculate the spectroscopic factors for cluster radioactivity. It should be mentioned that the fit to the data is not absolutely necessary. We use these values rather to compensate for eventual uncertainties in λ_G due to the WKB approximation and the choice of the potential (4). This increases the accurateness of our predictions slightly.

With the Gamov decay constant λ_G and the spectroscopic factor S , the absolute decay constant λ is estimated according to Eq. (2). Numerical values normalized to the experimental α -decay constants are listed in Table I for a number of selected decays. The measured branching ratios are reproduced up to a factor of 4, which may be considered as a typical error of our estimates. Known experimental limits are obeyed within the typical uncertainties. The unsuccessful search for ^{30}Mg and ^{34}Si decays is clearly explained by our results. The ^{14}C decays of ^{221}Ra , ^{221}Fr , and ^{225}Ac might be seen, if the detectable branching ratio can be decreased by an order of magnitude. The corresponding ratios predicted by the macroscopic model of Ref. 7 (Table II) are larger and not compatible with the experimental upper limits.

For many decays, our predictions and those of competing macroscopic models^{7,8} are not too different. In other cases, however, the results are in striking contrast as, e.g., for the heavier-cluster decays listed in Table II. In principle, experimentalists are in the position to make a clear decision in favor of one of these models.

The tunneling through the barrier made up by the fairly known outer trail of the potential is more or less unambiguous and common to all decay models, microscopic and macroscopic ones. The penetrability corresponding to this tunneling can be divided from the experimental decay rates according to Eq. (6). The various models differ then predominantly in the description of the "rest" (e.g., a factor of 10^{-10} for ^{14}C decay) which we call experimental spectroscopic factor. The so defined experimental spectroscopic factor was shown to possess a simple dependence on the mass number of the emitted cluster. In the microscopic model, with its pre-

TABLE I. Comparison of our order-of-magnitude estimates for $\lambda(a)$ with measured branching ratios for cluster radioactivity. All available data are reproduced within a factor of 4. Some predictions for as-yet unmeasured decay modes are also given.

$Z+z(A+a) \rightarrow {}^z a + {}^Z A$	$Q(a)$ (MeV)	$\lambda_{\text{expt}}(a)$ (s ⁻¹)	$\lambda(a)/\lambda_{\text{expt}}(a)$	$\lambda_{\text{expt}}(a)/\lambda_{\text{expt}}(a)$
${}^{222}\text{Ra} \rightarrow {}^{12}\text{C} + {}^{210}\text{Pb}$	29.16	1.8×10^{-2}	1×10^{-15}	...
${}^{221}\text{Ra} \rightarrow {}^{14}\text{C} + {}^{207}\text{Pb}$	31.39	2.4×10^{-3}	2×10^{-13}	$< 1.2 \times 10^{-13}$
${}^{222}\text{Ra} \rightarrow {}^{14}\text{C} + {}^{208}\text{Pb}$	33.16	1.8×10^{-2}	7×10^{-11}	3.7×10^{-10}
${}^{223}\text{Ra} \rightarrow {}^{14}\text{C} + {}^{209}\text{Pb}$	31.95	7.0×10^{-7}	8×10^{-10}	6.2×10^{-10}
${}^{224}\text{Ra} \rightarrow {}^{14}\text{C} + {}^{210}\text{Pb}$	30.64	2.2×10^{-6}	2×10^{-11}	4.3×10^{-11}
${}^{226}\text{Ra} \rightarrow {}^{14}\text{C} + {}^{212}\text{Pb}$	28.32	1.4×10^{-11}	4×10^{-11}	2.5×10^{-11}
${}^{221}\text{Fr} \rightarrow {}^{14}\text{C} + {}^{207}\text{Tl}$	31.39	2.4×10^{-3}	1×10^{-13}	$< 5.0 \times 10^{-14}$
${}^{225}\text{Ac} \rightarrow {}^{14}\text{C} + {}^{211}\text{Bi}$	30.58	8.0×10^{-7}	2×10^{-13}	$< 4.0 \times 10^{-13}$
${}^{224}\text{Th} \rightarrow {}^{14}\text{C} + {}^{210}\text{Po}$	33.06	6.7×10^{-1}	3×10^{-14}	...
${}^{226}\text{Th} \rightarrow {}^{14}\text{C} + {}^{212}\text{Po}$	30.67	3.7×10^{-4}	2×10^{-15}	...
${}^{224}\text{Th} \rightarrow {}^{16}\text{O} + {}^{208}\text{Pb}$	46.64	6.7×10^{-1}	1×10^{-15}	...
${}^{226}\text{Th} \rightarrow {}^{18}\text{O} + {}^{208}\text{Pb}$	45.88	3.7×10^{-4}	1×10^{-15}	...
${}^{228}\text{Th} \rightarrow {}^{20}\text{O} + {}^{208}\text{Pb}$	44.87	1.1×10^{-8}	4×10^{-14}	...
${}^{230}\text{Th} \rightarrow {}^{24}\text{Ne} + {}^{206}\text{Hg}$	57.96	2.9×10^{-13}	4×10^{-13}	5.6×10^{-13}
${}^{231}\text{Pa} \rightarrow {}^{24}\text{Ne} + {}^{207}\text{Tl}$	60.61	6.7×10^{-13}	4×10^{-12}	6.0×10^{-12}
${}^{232}\text{Th} \rightarrow {}^{24}\text{Ne} + {}^{208}\text{Hg}$	55.80	1.6×10^{-18}	5×10^{-11}	...
${}^{232}\text{U} \rightarrow {}^{24}\text{Ne} + {}^{208}\text{Pb}$	62.50	3.2×10^{-10}	4×10^{-12}	2.0×10^{-12}
${}^{233}\text{U} \rightarrow {}^{24}\text{Ne} + {}^{209}\text{Pb}$	60.69	1.4×10^{-13}	2×10^{-13}	7.6×10^{-13}
${}^{234}\text{U} \rightarrow {}^{24}\text{Ne} + {}^{210}\text{Pb}$	59.03	9.0×10^{-14}	2×10^{-13}	6.6×10^{-13}
${}^{232}\text{Th} \rightarrow {}^{26}\text{Ne} + {}^{206}\text{Hg}$	56.15	1.6×10^{-18}	2×10^{-12}	$< 5.0 \times 10^{-11}$
${}^{232}\text{Th} \rightarrow {}^{28}\text{Mg} + {}^{204}\text{Pt}$	69.64	1.6×10^{-18}	6×10^{-12}	...
${}^{234}\text{U} \rightarrow {}^{28}\text{Mg} + {}^{206}\text{Hg}$	74.35	9.0×10^{-14}	3×10^{-13}	2.2×10^{-13}
${}^{237}\text{Np} \rightarrow {}^{30}\text{Mg} + {}^{207}\text{Tl}$	75.24	1.0×10^{-14}	8×10^{-17}	$< 4.0 \times 10^{-14}$
${}^{240}\text{Pu} \rightarrow {}^{34}\text{Si} + {}^{206}\text{Hg}$	91.23	3.3×10^{-12}	8×10^{-17}	$< 1.3 \times 10^{-13}$
${}^{241}\text{Am} \rightarrow {}^{34}\text{Si} + {}^{207}\text{Tl}$	94.11	5.1×10^{-11}	2×10^{-19}	$< 5.0 \times 10^{-15}$

formation probability, this behavior is naturally understood supporting strongly the underlying model assumptions for the decay mechanism. In this picture the Pauli principle is responsible for the smallness of the spectroscopic factor $S \ll 1$. Although there is some success in phenomenological descriptions by macroscopic models, the neglect of the fermion character of the nucleons may cause some doubts on the reasoning of these models which also implicitly calculate a value corresponding to the

spectroscopic factor.

That the static microscopic model employed here seems to work even for rather heavy clusters is surprising. We are aware that this simple model, originally made for α decay, should break down somewhere when the mass number of the emitted fragment is further increased towards fission. Where this breakdown does occur, however, is difficult to tell.

We thank T. Fließbach for stimulating discussions.

TABLE II. For some branching ratios, our predictions and those of competing macroscopic models are not too incompatible. In other cases, however, the results are at variance.

$Z+z(A+a) \rightarrow {}^z a + {}^Z A$	Experiment	$\lambda(a)/\lambda(a)$		
		Present estimate	Macroscopic models (Ref. 7)	(Ref. 8)
${}^{221}\text{Ra} \rightarrow {}^{14}\text{C} + {}^{207}\text{Pb}$	$< 1.2 \times 10^{-13}$	2×10^{-13}	8.2×10^{-12}	6.3×10^{-13}
${}^{221}\text{Fr} \rightarrow {}^{14}\text{C} + {}^{207}\text{Tl}$	$< 5.0 \times 10^{-14}$	1×10^{-13}	8.0×10^{-12}	3.1×10^{-13}
${}^{225}\text{Ac} \rightarrow {}^{14}\text{C} + {}^{211}\text{Bi}$	$< 4.0 \times 10^{-13}$	2×10^{-13}	1.6×10^{-12}	6.3×10^{-13}
${}^{231}\text{Pa} \rightarrow {}^{24}\text{Ne} + {}^{207}\text{Tl}$	6.0×10^{-12}	4×10^{-12}	9.5×10^{-12}	1.0×10^{-10}
${}^{233}\text{U} \rightarrow {}^{24}\text{Ne} + {}^{209}\text{Pb}$	7.6×10^{-13}	2×10^{-13}	3.7×10^{-11}	2.0×10^{-11}
${}^{241}\text{Am} \rightarrow {}^{34}\text{Si} + {}^{207}\text{Tl}$	$< 5.0 \times 10^{-15}$	2×10^{-19}	...	4.0×10^{-13}

¹H. J. Rose and G. A. Jones, *Nature (London)* **307**, 245 (1984).

²P. B. Price, in *Frontiers of Heavy-Ion Physics*, edited by N. Cindro, W. Greiner, and R. Caplar (World Scientific, Singapore, 1987), p. 19, and references therein.

³T. Fliessbach and H. J. Mang, *Nucl. Phys.* **A263**, 75 (1976).

⁴R. Blendowske, T. Fliessbach, and H. Walliser, *Nucl. Phys.* **A464**, 75 (1987).

⁵The tunneling energy is given by $Q = (M_{A+a} - M_A - M_a)c^2$ where M_i are the masses of the bare nuclei. Since usually binding energies of neutral atoms are listed [A. H. Wapstra and G. Audi, *Nucl. Phys.* **A432**, 1 (1985)] one has to correct

for the (small) electronic binding energies [K. N. Huang, M. Aoyagi, M. H. Chen, B. Crasemann, and H. Mark, *At. Data Nucl. Data Tables* **18**, 243 (1976)]. Thereby the penetrability is increased up to a factor of 2 for the decays considered.

⁶P. R. Christensen and A. Winther, *Phys. Lett.* **65B**, 19 (1976).

⁷Y. J. Shi and W. J. Swiatecki, *Nucl. Phys.* **A438**, 450 (1985).

⁸D. N. Poenaru, W. Greiner, K. Depta, M. Ivascu, D. Mazilu, and A. Sandulescu, *At. Data Nucl. Data Tables* **34**, 423 (1986).